Electrical Power and Energy Systems 119 (2020) 105864

Contents lists available at ScienceDirect

Electrical Power and Energy Systems

journal homepage: www.elsevier.com/locate/ijepes

Accounting for reserve capacity activation when scheduling a hydropower dominated system

Christian Øyn Naversen[a,*], Hossein Farahmand[a], Arild Helseth[b]

[a] Department of Electric Power Engineering, Norwegian University of Science and Technology, 7491 Trondheim, Norway
[b] Department of Energy Systems, SINTEF Energy Research, Sem Sælands vei 11, 7034 Trondheim, Norway

ARTICLE INFO

Keyword:
Activation of reserved capacity
Hydropower scheduling
Hybrid stochastic-robust optimization

ABSTRACT

As the penetration of variable renewable power generation increases in power systems around the world, system security is challenged. It is crucial to coordinate the available flexible generating resources, such as hydropower, to meet the need for system balancing. However, reserved capacity on hydropower plants should only be activated if there is sufficient energy or storage capacity to either increase or decrease production. The potential change in production will also affect all reservoirs and plants connected by the cascaded topology. These issues are largely ignored or simplified in hydropower reserve scheduling models. To properly account for the possible activation of reserved capacity, several two-stage model formulations based on stochastic and robust optimization are presented and compared in this paper. The uncertainty in net load deviations due to forecasting errors in renewable power generation is considered the source of reserve capacity activation. The case study based on a real Norwegian watercourse clearly shows the benefit of using any of the two-stage model solutions over the standard deterministic reserve procurement. A novel hybrid stochastic-robust model formulation is presented and shown to efficiently increase the robustness of the solution without notably increasing the reserve procurement cost compared to the stochastic and robust models.

1. Introduction

Hydropower is a valuable asset for any power system, as it is flexible and fast to regulate compared to thermal generation technologies. As the share of variable renewable energy sources in power systems across the world increases, so does the need for balancing capacity and energy. Although hydropower is well suited to help balance the system, the technical constraints and cascaded topology must be considered to realistically estimate this balancing capability. A watercourse connects hydropower plants in space and time. Thus, the balancing actions of a single plant will impact the operation of the whole system, which is a challenge when considering spinning reserve capacity allocation. A hydropower plant delivering spinning reserve capacity in both directions must have sufficient stored water upstream to increase its production, and simultaneously it is beneficial to keep enough upstream storage capacity available to save unused water, in case the reserved capacity is activated upward or downward. The same is valid for the plants connected downstream of the activated plant since the water released has changed from its scheduled value. Another complicating aspect is the implicitly defined marginal cost of operating a hydropower plant. The stored water in each reservoir has an associated opportunity cost or water value, which in general depends on the stored water volumes. This makes the cost of procuring reserve capacity on a specific hydropower plant dependent on the capacity procured on the surrounding plants. Activating poorly coordinated reserve capacity in complex hydropower systems could lead to needless loss of potential energy and increased risk of load shedding.

Reserve capacity procurement and system balancing have been incorporated into hydropower scheduling models in several ways. These features can be found in both long-term planning models [21,13,14,1,18,20,28] and short-term operational models [24,23,9,15]. The fundamental models in [21,13,14] sequentially clear the day-ahead market, reserve procurement and system balancing steps for Northern Europe. The activation of reserve capacity is based on the marginal cost of the hydropower plants in their day-ahead position, but does not include hydrological constraints nor account for available energy in the reservoirs. The methods presented in [1] and [18] consider a producer participating in day-ahead energy and spinning reserve capacity markets under uncertainty in inflow and market prices within modified stochastic dual dynamic programming (SDDP) frameworks. Both methods ensure that enough water is stored in the reservoir to produce the allocated reserve capacity, although activation is not directly

* Corresponding author.
E-mail address: christian.naversen@ntnu.no (C.Ø. Naversen).

https://doi.org/10.1016/j.ijepes.2020.105864
Received 5 September 2019; Received in revised form 20 November 2019; Accepted 15 January 2020

Nomenclature

$\mathcal{L}$	robust uncertainty set
$\mathcal{I}_m^{d/b/o}$	modules that discharge/bypass/spill water into module m, index i
$\mathcal{J}$	robust worst-case scenarios, index j
$\mathcal{M}$	hydropower modules, index m
$\mathcal{N}_m$	discharge segments in module m, index n [A]
$\mathcal{S}$	balancing scenarios, index s
$\mathcal{T}$	time periods, index$t$
Ω	dual feasibility constraints for the balancing stage
$\mathcal{X}$	scheduling-stage feasibility constraints
$\mathcal{Y}$	balancing-stage feasibility constraints

Parameters

Δ^{max}	maximal net load deviation [MW]
Γ	budget of uncertainty
Λ_t	maximal hourly net load deviation in $\mathcal{L}$ [MW]
π_s	scenario probability
C^+	penalty for shedding load [mu/MW]
C^-	penalty for dumping power [mu/MW]
C^b	penalty for bypassing water [mu/m^3]
C^o	penalty for spilling water [mu/m^3]
E_{mn}	energy conversion factor [MWs/m^3]
F_t	length of time period [s]
I_{mt}	natural inflow [m^3/s]
L_t	forecasted system net load [MW]
P_m	maximal production capacity [MW]
Q_m^b	maximal flow through bypass gate [m^3/s]
Q_{mn}^d	maximal flow through discharge segment [m^3/s]
Q_m^o	maximal flow through spill gate [m^3/s]
R_t	system reserve requirement [MW]
T	number of time periods in $\mathcal{T}$
V_m^0	initial reservoir volume [m^3]
V_m	maximal reservoir capacity [m^3]
WV_m	end value of water [mu/m^3]

Variables

$\alpha^{\pm}$	auxiliary variables used in "big-M" formulation
Δ_t	net load deviation [MW]
λ_t	dual value of the power balance constraint in the balancing stage [mu/WMh]
θ	auxiliary variable approximating the value of the second-stage problem [mu]
ϕ	vector of all dual balancing-stage variables
$\mathbf{x}$	vector of all scheduling-stage variables
$\mathbf{y}$	vector of all balancing-stage variables
B	normalized system balancing cost [mu]
K	procurement cost of reserves [mu]
p_{mt}	generated hydropower [MW]
q_{mt}^b	flow through bypass gate [m^3/s]
q_{mnt}^d	flow through discharge segment [m^3/s]
q_{mt}^{in}	total controlled flow into reservoir [m^3/s]
q_{mt}^{out}	total controlled flow out of reservoir [m^3/s]
q_{mt}^o	flow through spill gate [m^3/s]
r_{mt}	symmetric spinning reserved capacity [MW]
s_t^+	load shedded [MW]
s_t^-	power dumped [MW]
U	normalized total system cost [mu]
u_t^+	load deviation in upward direction
u_t^-	load deviation in downward direction
v_{mt}	volume at the beginning of the time period [m^3]
W^{bal}	dual of second-stage objective function [mu]
Z^{bal}	second-stage objective function [mu]
Z^{da}	first-stage objective function [mu]

modelled. In [20], it is investigated how wind power can contribute to the provision of rotating reserves in a hydropower-dominated system by using the SDDP algorithm, but without considering reserve activation. The deterministic model presented in [24] has a high degree of physical detail and can model the reservation of all the different reserve capacity products in Norway. The total amount of reserve capacity to be allocated in the system is exogenously given to the model and is distributed among the hydropower plants while optimizing the day-ahead market position. The probability of activation in the balancing markets modifies the expected income in the deterministic model in [23], and the work in [9] is based on the assumption that a certain percentage of the reserve capacity sold to the market is activated by the system operator in every inflow and price scenario. The models in [28] and [15] do not explicitly model the reserve capacity procurement, but consider system balancing through bidding into the day-ahead, intraday and real-time energy markets.

This paper addresses the importance of explicitly representing the activation of reserved production capacity in the reserve procurement phase of a hydropower scheduling model. To the best of the authors' knowledge, this has not been addressed in detail in the literature before, and so emerges as a gap in the existing research. Related work on general energy storage devices exists to some degree. The stochastic unit commitment model with ideal energy storage in [36] balances load deviations by activating reserve capacity on thermal generators and energy storage devices. The model in [8] considers individual pumped storage plants coupled with thermal units, and energy constraints are applied to the reserve capacity procurement for extreme ramping scenarios that are decoupled in time. Bi-level complementarity models can be used to study the participation of an energy storage unit in day-ahead and reserve markets [33,35]. The work in [33] considers energy delivery in both the day-ahead and the real-time markets, but only satisfies the energy constraints of the storage units on average over a set of net load deviation scenarios. The bi-level energy storage investment model in [35] requires that there is sufficient storage and energy available to activate the reserved capacity at maximum for a single hour. The model presented in this paper differs from the general energy storage models in the representation of realistic and large-scale cascaded hydropower systems. To this end, note that short-term hydropower and hydrothermal scheduling is an active field of research, see for instance [25] and [12] for recent descriptions of state-of-the-art formulations.

The uncertain nature of variable renewable power generation and consumption contributes to the need for balancing services. Forecast errors in the net load of a power system force the system operator to activate reserved production capacity to meet the actual net load. There are several ways of modelling the uncertainty in net load deviations that cause the system to be unbalanced, such as stochastic and robust optimization. Stochastic optimization typically yields models which are risk neutral, while robust optimization hedges the solution against the worst-case realization of the uncertainty [6]. Robust optimization has been widely and successfully applied to power system planning and operation problems in recent years [32]. A large portion of the published scientific material has been related to the unit commitment problem under uncertainty, where the goal typically is to commit a sufficient number of thermal units to be able to balance real-time deviations [39]. These types of models are usually formulated as two-stage models [22,5,41,2,7], though single-stage [37] and multistage models [31,30] also exist. Robust optimization has also been used in the

context of hydropower scheduling under uncertainty, as in [3], where the energy content of the hydropower system is maximized while accounting for uncertain net load and inflow. In this paper, a combination of both the stochastic and robust modelling approaches are used to construct two-stage models that account for the effect of activation of reserve capacity in a hydropower system.

The combination of robust and stochastic optimization has been proposed in different ways. Stochastic and robust optimization may handle separate sources of uncertainty, such as generator availability and power prices in [11] and variable power generation and power prices in [27]. Moreover, it is possible to create hybrid models by taking a stochastic or a robust model and introducing some characteristics from the other approach. The work in [7] partitions the scenarios in a stochastic model into bundles where robust optimization is applied within each bundle, while [2] introduces several robust uncertainty sets to a robust model by weighting them in the objective function akin to scenario probabilities. The medium-term hydrothermal model presented in [38] procures reserve capacity to ensure system security in the face of a $N-k$ security criterion, which is done by incorporating robust optimization into the SDDP framework itself. The unified stochastic-robust model presented in [41] models the same source of uncertainty by both stochastic and robust optimization. This is done by introducing weight β of the average scenario cost and $1-\beta$ of the robust worst-case cost in the objective function, which represents a direct integration of both the stochastic and the robust optimization methods in a single problem. A novel hybrid model stochastic-robust model is presented in this paper, which leverages the popular column-and-constraint generation (CCG) solution technique (see [40,42]) as a scenario generator. The CCG provides robust scenarios for the mixed stochastic-robust model, which can be considered as extreme scenarios generated based on a robust uncertainty set. By tuning the probability given to these extreme scenarios, a model that is more robust without being overly conservative compared to its deterministic, robust, and stochastic counterparts is achieved. The complexity of the mixed stochastic-robust model is manageable, as the calculation of the robust scenarios is done before solving the complete model. In short, the contributions of this paper are considered twofold:

1. A new hybrid mixed stochastic-robust optimization model which is less complex in construction compared to other hybrid models is presented. In the numerical case study the new hybrid model improves the robustness of the solution without drastically increasing the cost compared to the pure robust and pure stochastic models.
2. The impact of considering activation of reserve capacity in complex and cascaded hydropower systems has been quantified.

The rest of the paper is organized into three parts: Section 2 details the modelling of the optimization problem formulations, a case study is presented in Section 3, and concluding remarks are found in Section 4. Section 2 is split into subsections describing the deterministic day-ahead scheduling problem (Section 2.1), the system balancing problem (Section 2.2), the stochastic and robust two-stage problems (Section 2.3), and the new mixed stochastic-robust problem (Section 2.4). The case study in Section 3 presents results from tuning the mixed stochastic-robust model (Section 3.2) and how the different model formulations compare (Section 3.3).

2. Modelling

The perspective taken in this paper is that of a system operator aiming at optimally scheduling and balancing a completely renewable system dominated by hydropower. The system is scheduled to be in balance according to the net load forecast in the day-ahead planning stage, and symmetric spinning reserve capacity is procured to ensure the balancing capabilities of the system. The existence of variable generation components in the system, such as wind and solar generation, is not modelled explicitly, but manifests as uncertainty in the net load. The forecast errors are seen as the main factors of this uncertainty, and are therefore the drivers behind the need for balancing services. The forecast errors in the net load become known after the scheduling step, and so the operator must use the procured reserve capacity to balance the system in the most efficient way possible.

2.1. Deterministic day-ahead scheduling problem

The deterministic short-term scheduling problem for the system operator,

$$\min_{\mathbf{x}} Z^{da}(\mathbf{x})$$
$$\mathbf{x} \in X, \tag{1}$$

aims to minimize the cost of using water to cover the required net load and spinning reserve requirements while respecting the physical constraints of the system. A standard linear definition of the hydropower scheduling problem, see for instance [19], is formulated as

$$\min_{\substack{v,p,r,\\ q^d,q^b,q^o,\\ q^{in},q^{out}}} \; -\sum_{m\in\mathcal{M}} WV_m v_{m,T+1} + \sum_{m\in\mathcal{M},t\in\mathcal{T}} F_t(C^b q^b_{mt} + C^o q^o_{mt}) \tag{2}$$

s.t.

$$v_{m0} = V^0_m \quad \forall\, m \in \mathcal{M} \tag{3}$$

$$q^{in}_{mt} = \sum_{i\in I^d_m, n\in\mathcal{N}_i} q^d_{int} + \sum_{i\in I^b_m} q^b_{it} + \sum_{i\in I^o_m} q^o_{it} \quad \forall\, m, t \in \mathcal{M}, \mathcal{T} \tag{4}$$

$$q^{out}_{mt} = \sum_{n\in\mathcal{N}_m} q^d_{mnt} + q^b_{mt} + q^o_{mt} \quad \forall\, m, t \in \mathcal{M}, \mathcal{T} \tag{5}$$

$$\frac{v_{m,t+1} - v_{mt}}{F_t} = I_{mt} + q^{in}_{mt} - q^{out}_{mt} \quad \forall\, m, t \in \mathcal{M}, \mathcal{T} \tag{6}$$

$$p_{mt} = \sum_{n\in\mathcal{N}_m} E_{mn} q^d_{mnt} \quad \forall\, m, t \in \mathcal{M}, \mathcal{T} \tag{7}$$

$$\sum_{m\in\mathcal{M}} p_{mt} = L_t \quad \forall\, t \in \mathcal{T} \tag{8}$$

$$p_{mt} + r_{mt} \le P_m \quad \forall\, m, t \in \mathcal{M}, \mathcal{T} \tag{9}$$

$$p_{mt} - r_{mt} \ge 0 \quad \forall\, m, t \in \mathcal{M}, \mathcal{T} \tag{10}$$

$$\sum_{m\in\mathcal{M}} r_{mt} \ge R_t \quad \forall\, t \in \mathcal{T} \tag{11}$$

$$0 \le v_{mt} \le V_m \quad \forall\, m, t \in \mathcal{M}, \mathcal{T}\cup\{T+1\} \tag{12}$$

$$0 \le q^d_{mnt} \le Q^d_{mn} \quad \forall\, m, n, t \in \mathcal{M}, \mathcal{N}_m, \mathcal{T} \tag{13}$$

$$0 \le q^b_{mt} \le Q^b_m \quad \forall\, m, t \in \mathcal{M}, \mathcal{T} \tag{14}$$

$$0 \le q^o_{mt} \le Q^o_m \quad \forall\, m, t \in \mathcal{M}, \mathcal{T} \tag{15}$$

$$0 \le p_{mt} \le P_m \quad \forall\, m, t \in \mathcal{M}, \mathcal{T} \tag{16}$$

All symbols in uppercase are input parameters to the model, while lowercase symbols represent the decision variables $\mathbf{x}$. The model is defined for the hydropower modules $m \in \mathcal{M}$ over the time periods $t \in \mathcal{T}$, where the terminology "hydropower module" is used to describe the combined unit of a reservoir connected to a power plant. The water may be moved between reservoirs through three different waterways: flow through the turbine, bypass gate, and spillage, see Fig. 1. The objective (2) of the model is to minimize the total cost of using water according to the water value and end volume of all reservoirs, as well as the small penalties for using the alternative bypass and spillage waterways. These penalties are applied to encourage the use of the main waterway through the plant. Water values represent the opportunity

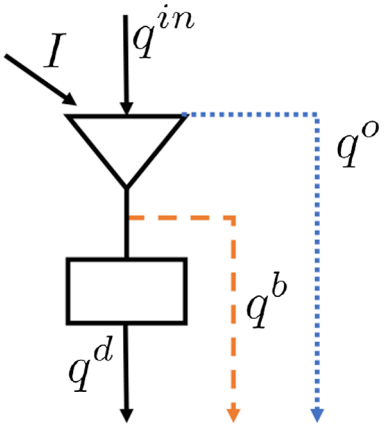

Fig. 1. Depiction of a hydropower module (reservoir and power plant) with different waterways for discharging, bypassing and spilling water.

cost of using water now versus storing it for later use, and are calculated by long-term models such as [19]. The end value of the water generally depends on the end volume in all reservoirs in the system, typically described by linear cutting planes. Constant water values are used in this model formulation for simplicity. Eqs. (3)–(6) preserve the water balance and topology between the modules in the system. The relation between water discharged through the turbine and the power produced by the generator is modelled as a piece-wise linear constraint in Eq. (7), where the efficiency is decreasing for increasing discharge segment number to ensure convexity of the problem. The power balance is kept by Eq. (8), while Eqs. (9) and (10) bound the available symmetric spinning reserve capacity of the plants. Note that the model is linear, which allows production down to 0 MW. To make sure the reserved capacity is spinning, the symmetric requirement is imposed. Enough reserve capacity must be allocated to satisfy the static reserve requirement in Eq. (11). Eqs. (12)–(16) are the bounds of the variables based on the physical capacities of the hydropower modules.

2.2. The balancing problem

Balancing the system in real time after a net load deviation Δ has occurred is necessary to maintain system stability. The decisions $\mathbf{x}$ made in the day-ahead scheduling stage will affect the system's ability to perform the balancing actions, and so the balancing problem

$$\begin{aligned} &\min_{\mathbf{y}} Z^{bal}(\mathbf{y}) \\ &\mathbf{y} \in \mathcal{Y}(\mathbf{x}, \Delta), \end{aligned} \tag{17}$$

depends on both $\mathbf{x}$ and Δ. The formulation is near identical to the day-ahead scheduling problem described by Eqs. (2) and (16) except for changes to Eqs. (2) and (8)–(10). All of the variable types found in Eqs. (2) and (16), except for the reserved capacity r, are found in $\mathbf{y}$ and have an analogous meaning. Let these variables be marked by an overline, so that $\bar{p}$ represents the power produced by a plant in the balancing stage and so on. The power balance constraint in Eq. (8) is augmented to include the net load deviation Δ as well as non-negative penalty variables for shedding load and dumping power:

$$\sum_{m \in \mathcal{M}} \bar{p}_{mt} + s_t^+ - s_t^- = L_t + \Delta_t. \quad \forall\, t \in \mathcal{T} \tag{18}$$

The penalty costs for using these penalty variables are added to the objective function formulation of Eq. (2),

$$\begin{aligned} Z^{bal}(\mathbf{y}) &= -\sum_{m \in \mathcal{M}} WV_m \bar{v}_{m,T+1} + \sum_{m \in \mathcal{M}, t \in \mathcal{T}} F_t (C^b \bar{q}^b_{mt} + C^o \bar{q}^o_{mt}) + \\ &\sum_{t \in \mathcal{T}} (C^+ s_t^+ + C^- s_t^-), \end{aligned} \tag{19}$$

and the production limits, Eqs. (9) and (10), are based on the procured spinning reserve capacity and production schedule in the day-ahead stage:

$$\bar{p}_{mt} \le p_{mt} + r_{mt} \quad \forall\, m, t \in \mathcal{M}, \mathcal{T} \tag{20}$$

$$\bar{p}_{mt} \ge p_{mt} - r_{mt} \quad \forall\, m, t \in \mathcal{M}, \mathcal{T} \tag{21}$$

The constraints defined in the day-ahead scheduling problem, Eqs. (3)–(7) and (12)–(16), are also included in the balancing problem constraints $\mathbf{y} \in \mathcal{Y}(\mathbf{x}, \Delta)$, but now pertaining to the balancing variables $\mathbf{y}$. The only connection to the decisions made in the day-ahead scheduling stage is through Eqs. (20) and (21).

2.3. Two-stage stochastic and robust problems

To account for the potential cost of activating the procured reserves in the scheduling phase, a two-stage model combining the day-ahead scheduling problem described in Section 2.1 with the system balancing problem in Sectin 2.2 is needed. In this section, two-stage problems based on traditional stochastic and robust optimization are formulated. The scheduling of production and procurement of reserve capacity is the first-stage problem, while balancing the system based on the first-stage solution and realized net load deviation Δ_t is considered as the second stage.

A stochastic problem is formulated by constructing a set $\mathcal{S}$ of balancing scenarios with net load deviations Δ_{st} and probabilities π_s, and then introducing a copy of the balancing problem (17) for each scenario into the deterministic scheduling problem (1). This leads to the extensive form of the classical two-stage stochastic problem formulation [32]:

$$\begin{aligned} &\min_{\mathbf{x}, \mathbf{y}_s} Z^{da}(\mathbf{x}) + \textstyle\sum_{s \in \mathcal{S}} \pi_s Z^{bal}(\mathbf{y}_s) \\ &\mathbf{x} \in \mathcal{X} \\ &\mathbf{y}_s \in \mathcal{Y}(\mathbf{x}, \Delta_s) \quad \forall\, s \in \mathcal{S}. \end{aligned} \tag{22}$$

The expected cost of balancing the system in all scenarios $s \in \mathcal{S}$ by activating the procured reserve capacity is minimized in this formulation, while also minimizing the cost of scheduling the system to meet the net load forecast and procuring the reserve capacity. The effect of activating the reserved capacity is properly captured in this model formulation, as constraints describing the cascaded hydropower topology and the energy usage of balancing the system are present in the balancing constraints. Note that the reserve capacity is activated for the whole time period t, which means the model does not distinguish between different types of reserves with different activation times.

The two-stage robust optimization formulation represents a more conservative approach than the stochastic formulation in Eq. (22). Robustness of the solution is of interest to the system operator, as keeping the system in balance, also in extreme situations, is a priority. The robust two-stage counterpart to the stochastic formulation is the tri-level problem

$$\begin{aligned} &\min_{\mathbf{x}} Z^{da}(\mathbf{x}) + \max_{\Delta} \min_{\mathbf{y}} Z^{bal}(\mathbf{y}) \\ &\mathbf{x} \in \mathcal{X} \\ &\Delta \in \mathcal{L} \\ &\mathbf{y} \in \mathcal{Y}(\mathbf{x}, \Delta), \end{aligned} \tag{23}$$

where the net load deviation Δ is constrained to be part of the uncertainty set $\mathcal{L}$. The robust problem aims to minimize the first-stage cost and the worst-case balancing cost. In this paper, the simple formulation first proposed in [4] will be used to define:

$$\mathcal{L}: =\{\Delta_t | \Delta_t = \Lambda_t \cdot (u_t^+ - u_t^-); \\ \sum_{t\in\mathcal{T}} (u_t^+ + u_t^-) \le \Gamma;\ u_t^\pm \in \{0, 1\}\}, \tag{24}$$

where the parameters Λ_t and Γ are the maximal net load deviation and the budget of uncertainty, respectively. The binary variables $u_t^\pm$ signify if a deviation in positive or negative direction has occurred. Note that it is possible to include both spatial and temporal correlations in the uncertainty set [29,30]. Since the distribution used to generate the scenarios for the stochastic model does not include any temporal correlations in the case study presented in Section 3, correlations are not included in the uncertainty set.

The min-max-min formulation of the robust optimization problem in Eq. (23) cannot be solved directly. The column-and-constraint generation (CCG) procedure, first proposed in [40,42], is a popular primal decomposition scheme to remedy this. Other solution techniques such as Benders decomposition (see for instance [5]) and affine policy approximation [31,30] are not considered in this work because the model presented in Section 2.4 depends on the CCG approach. CCG first requires the inner minimization problem of Eq. (23) to be transformed to its dual maximization form, so that the maximization steps may be combined:

$$\max_{\Delta\in\mathcal{L}} \min_{\mathbf{y}} Z^{bal}(\mathbf{y}) \ \Leftrightarrow \ \max_{\Delta\in\mathcal{L},\phi} W^{bal}(\mathbf{x}, \Delta, \phi) \\ \mathbf{y} \in \mathcal{Y}(\mathbf{x}, \Delta) \qquad \phi \in \Omega. \tag{25}$$

Let the dual variables of the power balance constraints in the balancing stage, Eq. (18), be denoted as λ_t. Bi-linear terms $\Delta_t\lambda_t = \Lambda_t \cdot (u_t^+\lambda_t - u_t^-\lambda_t)$ appear in the objective function W^{bal} when Eq. (18) is dualized. The binary definition of Δ_t in Eq. (24) allows for an exact reformulation of the bi-linear problem to a mixed integer linear program (MILP) by using a "big-M" approach. This is done in for instance [22], though other options are available for solving the problem. An alternating direction method was used in [29], while a cutting plane outer approximation was implemented in [5]. In this paper the exact MILP reformulation will be used, as it can be solved directly with a standard MILP solver. With the introduction of the penalty costs $C^\pm$ for shedding load and dumping power in Eq. (19) through the non-negative variables $s_t^\pm$, the dual variables λ_t will be constrained by these values:

$$-C^- \le \lambda_t \le C^+ \qquad \forall\, t \in \mathcal{T}. \tag{26}$$

Using the bounds on λ_t in the big-M expansion allows the bi-linear terms $\pm\, u_t^\pm\lambda_t$ to be replaced by the new variables $\alpha_t^\pm$ and the additional constraints

$$\alpha_t^+ \le \lambda_t + C^-(1 - u_t^+) \qquad \forall\, t \in \mathcal{T} \tag{27}$$

$$\alpha_t^+ \le C^+ u_t^+ \qquad \forall\, t \in \mathcal{T} \tag{28}$$

$$\alpha_t^- \le -\lambda_t + C^+(1 - u_t^-) \qquad \forall\, t \in \mathcal{T} \tag{29}$$

$$\alpha_t^- \le C^- u_t^- \qquad \forall\, t \in \mathcal{T}. \tag{30}$$

The CCG technique is based on repeatedly solving the dual form of Eq. (25) for iteratively updated first-stage solutions $\mathbf{x} \in \mathcal{X}$. The solution yields the realization of the worst-case net load deviation Δ_j, which is iteratively added to the master problem

$$\min_{\mathbf{x},\mathbf{y}_j,\theta} Z^{da}(\mathbf{x}) + \theta \\ \mathbf{x} \in \mathcal{X} \\ \theta \ge Z^{bal}(\mathbf{y}_j) \qquad \forall\, j \in \mathcal{J} \\ \mathbf{y}_j \in \mathcal{Y}(\mathbf{x}, \Delta_j) \qquad \forall\, j \in \mathcal{J}. \tag{31}$$

The set $\mathcal{J}$ represents the worst-case net load deviation scenarios that have been identified by the inner maximization problem, and the auxiliary variable θ is an outer approximation of Eq. (25). Solving the master problem results in an updated first-stage solution $\mathbf{x}$, which is used to solve Eq. (25) in the next iteration. When the current value of θ and W^{bal} have converged within a specified tolerance, the procedure is complete as the optimal solution of Eq. (23) has been found.

2.4. Mixed stochastic-robust problem

In an effort to combine the advantages of the stochastic and the robust problem formulations presented in Section 2.3, a novel mixed stochastic-robust formulation that utilizes the solution of the pure robust problem formulated in Eq. (23) is proposed here. Solving the robust problem with the CCG algorithm results in a set of worst-case net load deviations $\mathcal{J}$, as explained in Section 2.3. These deviations are realizations of the net load that maximizes the cost of balancing the system in the robust formulation. Therefore, the CCG algorithm can be seen as a generator of extreme scenarios that are contained within the uncertainty set $\mathcal{L}$. The mixed stochastic-robust model is formed in Eq. (32) by extending the stochastic problem formulation in Eq. (22) with the set of robust scenarios:

$$\min_{\mathbf{x},\mathbf{y}_s,\mathbf{y}_j} Z^{da}(\mathbf{x}) + \sum_{s\in\mathcal{S}} \pi_s^* Z^{bal}(\mathbf{y}_s) + \sum_{j\in\mathcal{J}} \pi_j Z^{bal}(\mathbf{y}_j) \\ \mathbf{x} \in \mathcal{X} \\ \mathbf{y}_s \in \mathcal{Y}(\mathbf{x}, \Delta_s) \qquad \forall\, s \in \mathcal{S} \\ \mathbf{y}_j \in \mathcal{Y}(\mathbf{x}, \Delta_j) \qquad \forall\, j \in \mathcal{J}. \tag{32}$$

Note that the probabilities of the original scenarios $s \in \mathcal{S}$ have been scaled so that

$$\sum_{s\in\mathcal{S}} \pi_s^* + \sum_{j\in\mathcal{J}} \pi_j = 1. \tag{33}$$

All original scenarios are scaled down with the same factor $0 \le \beta \le 1$,

$$\pi_s^* = \beta\pi_s \qquad \forall\, s \in \mathcal{S}. \tag{34}$$

The robust scenarios are considered to be equiprobable, which results in the robust probabilities

$$\pi_j = (1 - \beta)/|\mathcal{J}| \qquad \forall\, j \in \mathcal{J}. \tag{35}$$

Choosing a scaling of $\beta = 1$ will put zero weight on the robust scenario balancing costs, and similarly $\beta = 0$ removes the cost of balancing the original scenarios. The constraints $\mathcal{Y}(\mathbf{x}, \Delta)$ associated with the original and robust scenarios will persist regardless of the choice of β. The formulation in Eq. (32) is similar to the unified stochastic-robust model in [41], as the robust and stochastic components of the problem is weighted in the objective function in both models. However, there are two main differences between Eq. (32) and other hybrid models;

Firstly, the robust scenarios $\mathcal{J}$ are computed by solving the robust model in Eq. (23) before the mixed model is solved. In contrast, the unified stochastic-robust model must be solved in an iterative way with the presence of the scenarios $\mathcal{S}$ in every iteration, which can be problematic regarding the tractability of the problem. The mixed model presented here may be solved directly in its extensive form, or by any other suitable decomposition technique for stochastic optimization problems. The reusability of the robust scenarios $\mathcal{J}$ are also higher in the mixed model formulation since they are completely independent of the original scenarios $\mathcal{S}$. For instance, if the mixed model is solved for successive days, the scenarios $\mathcal{J}$ can be used as a good initial set of constraints in the solution of the robust model. This sharing of contingency events between time periods has also been proposed for the long-term hydrothermal planning model in [38], which incorporates CCG in a SDDP framework.

The second important difference is that the expected value of the robust scenarios is added to the objective function in Eq. (32) instead of the max-min robust formulation. If only the maximal cost of the robust scenarios was minimized, the mixed model would be little more than an approximation of the unified model of [41] with pre-generated robust scenarios. As pointed out in Section 2.2, the only direct connections between the first and second stages are the production limits Eqs. (20) and (21). For the hydropower scheduling problem, this turns out to be a

very weak coupling in the sense that including the constraints $\mathbf{y} \in \mathcal{Y}(\mathbf{x}, \Delta)$ alone do not have a big impact on the first-stage decisions. It is important to include the balancing cost $Z^{bal}(\mathbf{y})$ of a scenario to the objective function to actually influence the scheduling decisions. This effect is clear in the numerical calculations in Section 3.2 for the edge case $\beta = 1$. Directly including all robust scenarios in the objective function through their expected cost instead of only minimizing the maximal balancing cost leads to a tighter connection between the stages, and a more efficient way of propagating the conservative nature of the robust scenarios to the reserve capacity procurement decision. The coupled model proposed in [26] also minimizes the expected value of robust scenarios, but in their case the robust scenarios are iteratively added to the set $\mathcal{S}$ through the CCG procedure. The approach still has the potential tractability issues of the unified problem formulation, especially since the convergence of the CCG algorithm is unproven in their proposed framework.

3. Case study

The focus of this case study is on the quality of the solution of the deterministic, stochastic, robust, and mixed model formulations presented in Section 2. The solution quality is measured in terms of the cost of procuring the reserve capacity and the subsequent cost of activating the reserves to balance the system. The topic of solution times of the different models is not discussed directly, as this will be heavily dependent on the solution parameters and techniques used to solve the models, especially the robust and, by extension, the mixed models. All optimization models have been implemented in the Pyomo modelling package for Python [16,17] using the MILP solver CPLEX 12.8 [10].

The hydropower system used in the study is shown in Fig. 2. It is based on a real watercourse in Norway, and consists of 12 modules with a total production capacity of 537.4 MW. The initial reservoir volume of every module is set to 65% of its maximal storage capacity, which represents a normal hydrological situation during the winter in Norway. Water values are calculated by the long-term hydropower scheduling model described in [19], and are measured in monetary units (mu) per Mm^3 in the range of 1200–9000 mu/Mm^3. The penalty for shedding load and dumping power is chosen to be 3000 mu/MW and 1000 mu/MW, respectively. Note that the results in the case study is not overly affected by the choice of these values due to the way the net load deviation scenarios are generated. The time horizon is set to 24 h with hourly resolution, and the forecasted net load profile is shown in Fig. 3. The profile is based on the amount of energy sold in the day-ahead market in the Norwegian NO3 bidding zone on 1/1-2019 [34], with values scaled down to get a peak of 420 MW. The maximal forecast error possible is considered to be $\Delta^{max} = 42$ MW, 10% of the peak load, in either direction in every hour. No temporal correlations between net load forecast errors are assumed for simplicity.

To generate scenarios for the stochastic and mixed models, the forecast errors Δ_t are chosen to be normally distributed with $\mu_t = 0$ and $\sigma_t = \Delta^{max}/2.5 = 16.8$ MW. However, to ensure that the values drawn to generate the scenarios are within the postulated maximal forecast error band, any values outside this band are truncated to its outer limits. In other words, $|\Delta_{st}| \leq \Delta^{max}$ is enforced for all scenarios.

There are two measures that are used to quantify the quality of a production and reserve capacity procurement schedule; The cost of procuring the reserves K and the following cost of balancing the system B. The cost of procuring reserves is defined as the increase in the first-stage objective function Z^{da} relative to the cost of the deterministic model in Eq. (1) solved without any reserve requirement, Z_0^{da}:

$$K = Z^{da} - Z_0^{da}. \tag{36}$$

This cost represents the opportunity cost of procuring the reserves. For a given realization of the net load deviation Δ_i, the cost B_i of balancing this deviation is calculated by solving the primal balancing problem in Eq. (17) for the given production schedules p and allocated reserve capacity r. This yields the objective function Z_i^{bal}, which is normalized by the objective function given perfect foresight, Z_i^{PF}, to produce the balancing cost:

$$B_i = Z_i^{bal} - Z_i^{PF}. \tag{37}$$

The perfect foresight cost is found by relaxing the production limit constraints of the balancing problem, Eqs. (20) and (21), to let every plant produce between zero and maximum capacity. The sum of the procurement cost and the normalized balancing cost is the total system cost,

$$U_i = K + B_i. \tag{38}$$

K is easily found by direct calculation, whereas the balancing costs B_i must be estimated by simulation. In this case study, 5000 different sampled net load deviations were used to measure the balancing cost of the given schedule. The robustness of the different model solutions was tested by generating two different batches of 5000 balancing scenarios. The first batch, from now on referred to as "the normal scenario batch", was generated based on the same truncated normal distribution used when generating scenarios for the stochastic and mixed models. A different seed for the random number generator was used when generating the normal scenario batch to avoid redrawing the same scenarios generated for the solution of the stochastic and mixed models. The second batch of scenarios was generated from a uniform distribution drawing values in the range $|\Delta_t| \leq \Delta^{max}$. This uniform scenario batch gives balancing scenarios that are more extreme compared to the normal scenario batch. The system is guaranteed not to experience any net load deviation larger than Δ^{max} in any of the scenarios in the two batches, and so penalties for load shedding and dumping power can be avoided given that enough energy and storage capacity is available when the reserves are activated.

3.1. Sensitivity analysis of the budget of uncertainty in the robust model

The parameters of the robust uncertainty set $\mathcal{L}$ are chosen to be comparable to the scenarios generated from the truncated normal distribution. The maximal deviation is set to $\Lambda_t = \Delta^{max}$ so that the worst-case deviation contained in $\mathcal{L}$ does not exceed the maximal hourly net load deviation. The budget of uncertainty Γ heavily influences the solution of the robust model. According to the formulation in Eq. (24), Γ limits the maximal number of hours with a worst-case deviation. To gauge the robustness of the solution of the robust model in Eq. (23), a sensitivity analysis of Γ in the range from 1 to 24 was performed. The robust model was solved for the 24 different values of Γ to an absolute

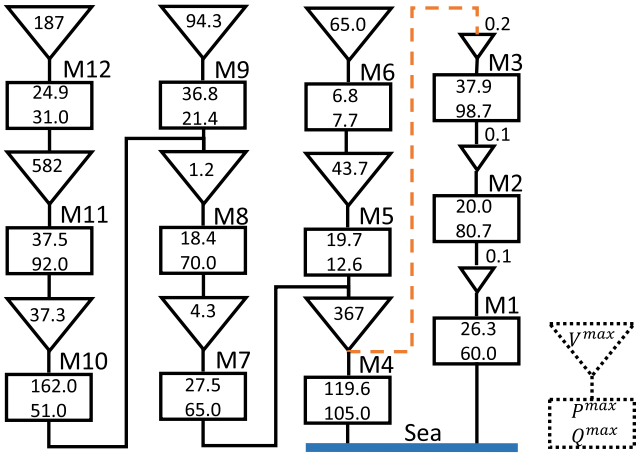

Fig. 2. Sketch of the hydropower topology. Reservoirs (triangles), power plants (rectangles), and water routes for discharge (solid lines) and bypass (dashed line) are shown together with maximal values for discharge (m^3/s), production (MW) and reservoir volumes (Mm^3).

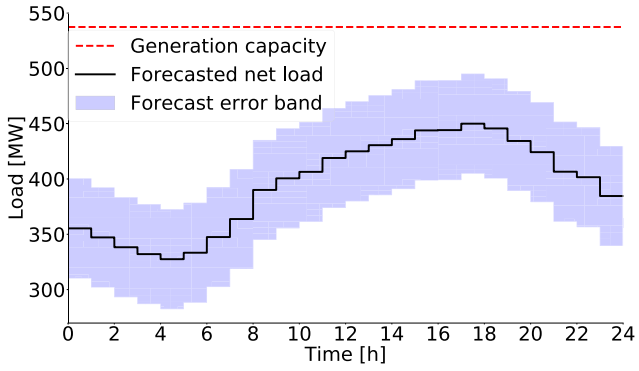

Fig. 3. Forecasted system net load with the region of possible deviations and the total generation capacity of the system.

convergence tolerance of 5 mu, with an absolute MIP gap of 5 mu and integer tolerance of 10^{-9} for the second-stage problem. The CCG algorithm on average converged in 15 iterations, and always within 29 iterations. The procurement cost K was determined based on Eq. (36) and balancing cost B_i was then calculated for all of the scenarios in the normal and uniform scenario batches according to Eq. (37). The numerical results are shown in Fig. 4.

The sensitivity analysis shows that the value of Γ has a big impact on both the procurement cost and simulated balancing cost of the robust model. As expected, K increases almost monotonically as a function of Γ. The balancing cost is generally higher for low values of Γ for both batches of simulation scenarios, but the trend is not monotone. There is a distinct drop in the variability of B_i for $\Gamma > 10$, but the variability starts to increase again when close to the maximal value of $\Gamma = 24$. This shows that simply choosing a high budget of uncertainty does not necessarily result in a more robust solution. Fig. 4 shows that choosing $\Gamma = 1$ results in the lowest average total cost U^{mean} when simulating with the normal scenario batch but the highest U^{mean} in the uniform scenario batch. In terms of robustness, the best choice is arguably $\Gamma = 15$. The 95th percentile of the total cost is lowest for this value of Γ for both simulation scenario batches, and its average total cost is also the lowest in the uniform scenario batch.

3.2. Sensitivity analysis of the robust weight βb in the mixed stochastic-robust model

The scaling factor β of the mixed stochastic-robust model in Eq. (32) is considered a tuning parameter in this case study, and its optimal value is estimated in this section based on a similar type of sensitivity analysis as in Section 3.1. It was determined that $\Gamma = 15$ gave the most robust solution when the pure robust model was considered, which was reached after 12 iterations of the CCG algorithm. The corresponding 12 robust scenarios form the set $\mathcal{J}$ for the mixed model. An additional 50 equiprobable scenarios were generated to form the set $\mathcal{S}$ of balancing scenarios based on the truncated normal distribution described in Section 3. The mixed model was solved for a range of different values of β to find the procurement cost K before the balancing cost B_i was simulated based on the 5000 scenarios in the normal and the uniform scenario batches. The numerical results are visualized in Fig. 5. When determining the range of β to consider in the mixed model, it is useful to calculate the value of β that results in equal weights for the scenarios in $\mathcal{S}$ and $\mathcal{J}$. Based on Eqs. (34) and (35), this value is

$$\beta_0 = \frac{|\mathcal{S}|}{|\mathcal{S}| + |\mathcal{J}|} \approx 0.806 \tag{39}$$

given the number of robust and regular scenarios used. A value of $\beta < \beta_0$ will result in a mixed model where the individual robust scenarios are given a higher weight than the scenarios in $\mathcal{S}$, which is likely to give an overly conservative solution. This turned out to be true in this case study, so only values in the range $0.8 \leq \beta \leq 1.0$ are presented in this analysis.

The results show that a lower value of β gives a lower standard deviation $\sigma(U_i)$ at the expense of a higher base procurement cost K. Interestingly, the standard deviation increases noticeably for the edge case $\beta = 1$. Only adding the constraints related to the balancing problem without considering the associated balancing cost in the objective causes this effect, and the balancing constraints alone do not impact the model sufficiently to increase its robustness. The value of β that achieves the lowest average total cost is 0.99 and 0.91 when using the normal and uniform simulation scenario batches, respectively. The most robust solutions occur at $\beta = 0.93$ and $\beta = 0.84$ in the two simulation cases when the 95th percentile of the total cost as a measure for robustness. This finding shows that it is possible to gain both robustness and lower average costs at the same time by adding robust scenarios to a stochastic optimization problem. The "best" choice of β depends on the preferences of the system operator, and most choices in the region $0.84 \leq \beta \leq 0.99$ can be justified based on a trade-off between robustness and low average cost. However, it is clear that giving zero weight to the robust scenarios ($\beta = 1$) is a sub-optimal choice either way.

3.3. Model comparison

To compare the mixed model and the robust model with the deterministic (Eq. (1)) and stochastic (Eq. (22)) formulations, the same simulation run of 5000 balancing scenarios drawn from the truncated normal distribution and the uniform distribution was used to simulate

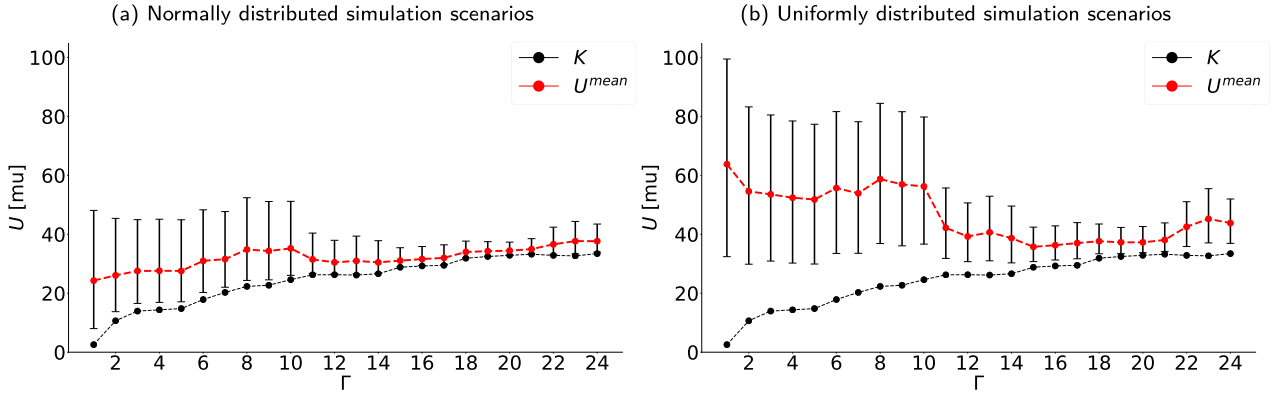

Fig. 4. Cost simulation for the robust model solution for different values of Γ. The simulation in (a) used balancing scenarios drawn from a normal distribution, while (b) used uniformly distributed scenarios. The procurement cost and the average total cost are shown as black and red points, respectively. The 5th and 95th percentiles of the total cost are shown as error bars for each value of Γ. (For interpretation of the references to colour in this figure legend, the reader is referred to the web version of this article.)

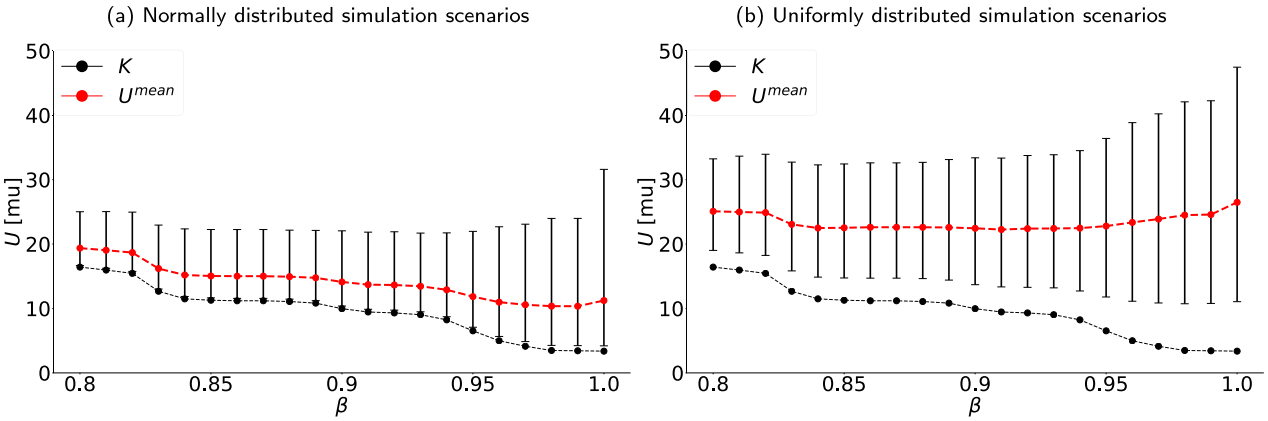

Fig. 5. Cost simulation for the robust model solution for different values of β. The simulation in (a) used balancing scenarios drawn from a normal distribution, while (b) used uniformly distributed scenarios. The procurement cost and the average total cost are shown as black and red points, respectively. The 5th and 95th percentiles of the total cost are shown as error bars for each value of β. (For interpretation of the references to colour in this figure legend, the reader is referred to the web version of this article.)

the costs. The deterministic model was solved with a static reserve requirement of $R_t = \Delta^{max} = 42$ MW. The stochastic model was solved with 50, 200 and 1000 scenarios drawn from the truncated normal distribution, where the 50 first scenarios are identical to the ones used in the mixed model. The results of the simulation are shown in Fig. 6 with accompanying numerical details given in Table 1. There are no instances of load shedding or power dumping penalties being used in any of the simulation runs for any of the models.

The first observation to note is the advantage of considering the activation of reserves in a cascaded hydropower system. The deterministic model procures the 42 MW of reserve capacity and does not shift the production schedule of any module from the schedule obtained when not procuring reserve capacity. This gives a low procurement cost of $K = 0$, but it is evident that the cost of actually balancing the system after the net load has been realized is high compared to all of the two-stage models. The average cost is 7–8 times higher for the deterministic model solution compared to the stochastic and mixed model solutions. The robust model with $\Gamma = 15$ is considered overly conservative in this comparison due to a high procurement cost. Note that the least conservative robust model with $\Gamma = 1$, see Fig. 4, also performs significantly worse than the other two-stage models. The stochastic model with 50 scenarios performs well in the simulation using the normal scenario batch but has high variability in the balancing cost and low robustness when the simulation is based on the uniform scenario batch. By increasing the number of scenarios in the stochastic model to 200 and 1000, the average total cost, variability, and robustness improve.

Table 1
Numeric values of the procurement cost, average total cost, 95th percentile of the total cost and the standard deviation of the total cost for the different model formulations. The simulation in (a) used balancing scenarios drawn from a normal distribution, while (b) used uniformly distributed scenarios.

(a) Normally distributed simulation scenarios

Model	K	U^{mean}	$U^{95\%}$	$\sigma(U_i)$
Deterministic	0.00	84.69	144.65	32.99
Robust, $\Gamma = 15$	28.82	31.06	35.45	2.11
Stochastic, 50 scen.	3.37	11.24	31.60	8.24
Stochastic, 200 scen.	3.12	10.06	23.11	6.58
Stochastic, 1000 scen.	3.11	9.72	21.99	5.91
Mixed, $\beta = 0.84$	11.50	15.19	22.36	3.37
Mixed, $\beta = 0.99$	3.43	10.35	23.99	6.23

(b) Uniformly distributed simulation scenarios

Model	K	U^{mean}	$U^{95\%}$	$\sigma(U_i)$
Deterministic	0.00	208.92	300.38	51.52
Robust, $\Gamma = 15$	28.82	35.74	42.44	3.59
Stochastic, 50 scen.	3.37	26.50	47.46	11.38
Stochastic, 200 scen.	3.12	24.38	42.31	9.82
Stochastic, 1000 scen.	3.11	23.68	40.48	9.28
Mixed, $\beta = 0.84$	11.50	22.49	32.29	5.42
Mixed, $\beta = 0.99$	3.43	24.58	42.25	9.58

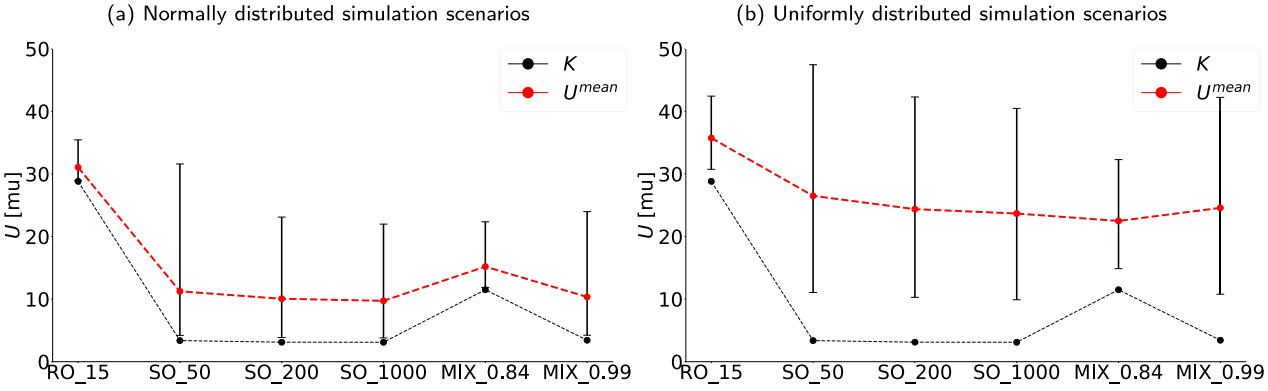

Fig. 6. Cost simulation comparing the robust, stochastic and mixed model solutions. The simulation in (a) used balancing scenarios drawn from a normal distribution, while (b) used uniformly distributed scenarios. The procurement cost and the average total cost are shown as black and red points, respectively. The 5th and 95th percentiles of the total cost are shown as error bars for each model. (For interpretation of the references to colour in this figure legend, the reader is referred to the web version of this article.)

However, this comes at the expense of model size and complexity, and the marginal improvement per scenario is low when going from 200 to 1000 scenarios. The mixed model only adds 12 new scenarios, but still manages to provide robust solutions without being overly conservative. The mixed model with $\beta = 0.84$ yields the most resilient solution when simulating with the uniform scenario batch, with a 95th percentile cost that is considerably lower than the other models. The increased procurement cost results in a higher average total cost in the normal scenario batch simulation, but the 95th percentile cost is still only slightly higher than the stochastic model with 1000 scenarios. When the mixed model is solved with $\beta = 0.99$, the result is a model which behaves similarly to the stochastic model with 200 scenarios. This model comparison shows that using robust scenarios in a stochastic model can drastically reduce the number of scenarios needed to improve robustness and average total cost.

To better understand the effect and importance of considering reserve capacity activation in the scheduling phase, Fig. 7 shows how some of the different models allocate and distribute the reserve capacity among the 12 hydropower plants. The deterministic model relies heavily on plant 4 for reserve capacity throughout the day, and fills the remaining reserve capacity need with reserves arbitrarily allocated on other plants that operate between 0 and P^{max}. There is no spatial coordination between plants that are selected for reserving capacity in the deterministic model. In this case, module 4 has ample energy stored upstream and additional storage space to ramp up or down production without issue, but this is purely by chance. The module is also located at the bottom of the cascaded system, and so any change in water discharged does not cause problems downstream. As seen in Table 1, the deterministic reserve procurement still turns out to be costly when it comes to balancing the system. Using plant 4 to balance most of the net load deviations results in poor water management according to the water values. All of the two-stage models also rely on plant 4 for their reserve capacity, but to a lesser extent. The shape of the forecasted net load curve, with a valley in hours 2–6 and a peak in hours 14–20, can be seen in the allocation of the reserve capacity, which reflects the fact that it is better to use different hydropower modules for balancing at different times of the day. Modules 1, 2 and 3 are located in a string with very limited storage capacity and are used for reserve capacity during the peak hours. Reserve capacity is allocated on these plants at the same time so that they can ramp up or down together to avoid issues caused by the low storage capacity in between them. The robust model allocates significantly more reserve capacity on plants 1, 2 and 3 compared to the stochastic and mixed models. This forces an increased use of the bypass gate from module 4 to module 3 to feed the three modules with additional water so that they can increase their production and deliver more spinning reserve capacity. Using the bypass gate incurs a small penalty, which increases the procurement cost of the robust model. It is clear that the robust model values protection in the peak hours. The worst-case system costs occur when positive deviations manifest in the peak hours since this forces the hydropower system to produce closer to its maximal capacity. The mixed model with $\beta = 0.84$ inherits the protection of the peak hours. It procures between 50 and 55 MW of reserve capacity in several hours in the peak period, which is over the necessary 42 MW to avoid load shedding and power dumping. The additional reserve capacity gives increased flexibility in the balancing stage, as different combinations of modules can be used to produce or retain the required balancing energy, even in the case where a maximal net load deviation is realized. Except for the peak hours, the stochastic and mixed models produce a similar reserve capacity procurement. This is to be expected since most of the weight is still allocated to the scenarios used in the stochastic model.

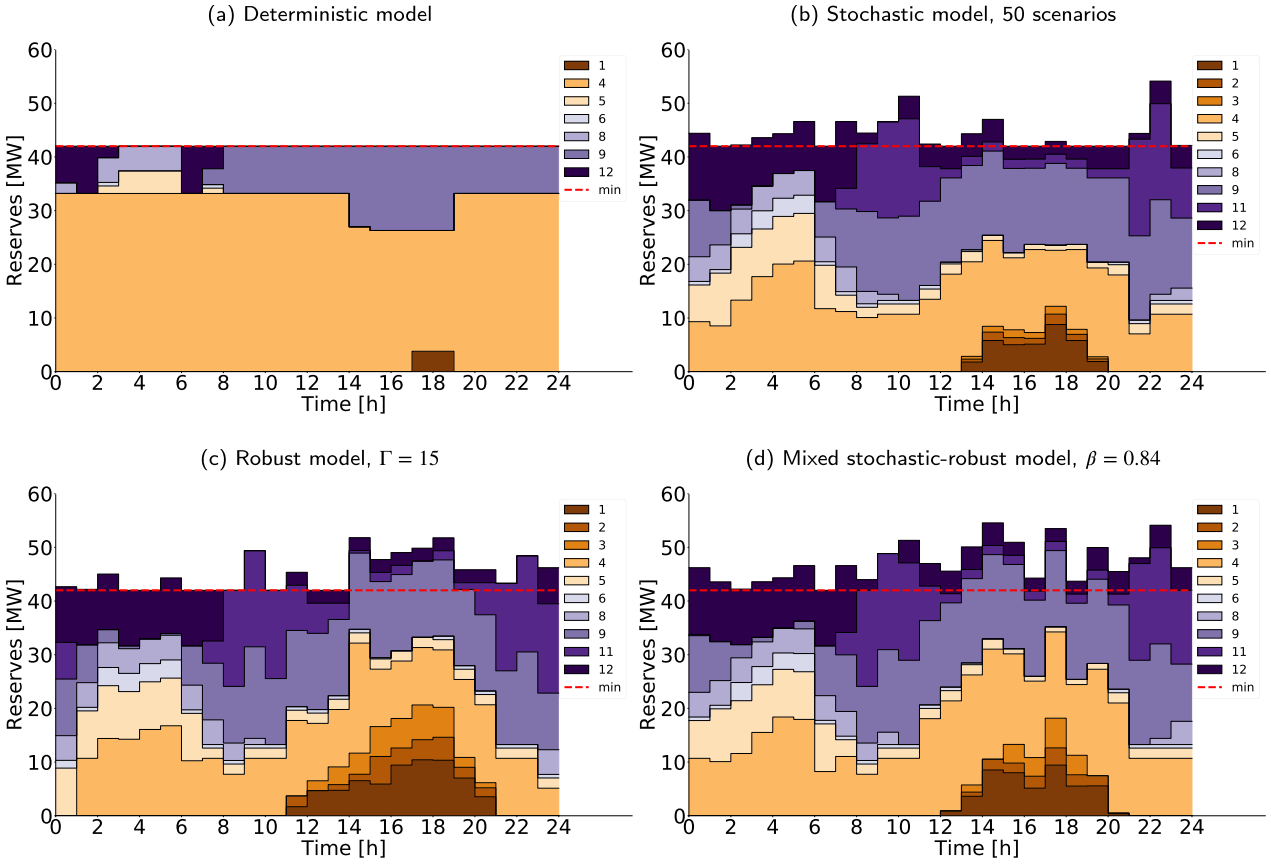

Fig. 7. Reserve allocation on the 12 hydropower modules for the different models. The minimal reserve required to avoid load shedding is shown as a red dashed line. (For interpretation of the references to colour in this figure legend, the reader is referred to the web version of this article.)

4. Conclusion

In this paper, the importance of considering the activation of reserved capacity in the scheduling phase for hydropower has been highlighted. If activation is not considered, having sufficient amounts of both stored energy and energy storage capacity can become issues in real-time operations. Cascaded hydropower systems have the added problem of being physically connected, and therefore, many plants will be affected by a single plant ramping up and down its production. In the presented case study, inefficient water management was the source of the high balancing cost of the deterministic model. Several two-stage formulations, which considers activation of reserves in combination with energy and topology constraints in the balancing stage, were proposed to solve this issue. One of these models is a new mixed stochastic-robust optimization model, which was shown to yield high-quality solutions compared to its pure stochastic and pure robust model ancestors. The mixed model can be viewed as a stochastic model augmented with extreme scenarios identified by solving a robust model with the CCG algorithm. The fact that a non-zero robust weight minimizes the total costs in the mixed model signifies a benefit of strengthening the stochastic model with robust scenarios. This is especially valid when the probability distribution used to generate the scenarios for the stochastic model is different from the actual distribution of the uncertainty, which can be the case when the underlying data is of poor quality.

The case study presented in this paper is based on a moderate case regarding the initial state and energy available in the system. Solving the daily scheduling problem over a longer period that captures the seasonal variations in the hydropower system, for instance by using a rolling horizon simulator, will give a complete picture of the effects of spatially coordinating the reserve capacity allocation based on accounting for activation.

CRediT authorship contribution statement

Christian Øyn Naversen: Writing - original draft, Methodology, Conceptualization, Software, Formal analysis, Data curation, Visualization. **Hossein Farahmand:** Conceptualization, Writing - review & editing, Supervision. **Arild Helseth:** Conceptualization, Writing - review & editing, Project administration, Funding acquisition, Supervision.

Declaration of Competing Interest

The authors declare that they have no known competing financial interests or personal relationships that could have appeared to influence the work reported in this paper.

Acknowledgements

This work was funded by The Research Council of Norway, Project No. 268014/E20.

References

[1] Abgottspon Hubert, Njálsson Karl, Bucher Matthias A, Andersson Göran. Risk-averse medium-term hydro optimization considering provision of spinning reserves. 2014 int. conf. probabilistic methods appl. to power syst. IEEE; 2014. p. 1–6. https://doi.org/10.1109/PMAPS.2014.6960657. ISBN 978-1-4799-3561-1.

[2] An Yu, Zeng Bo. Exploring the modeling capacity of two-stage robust optimization: variants of robust unit commitment model. IEEE Trans Power Syst 2015;30(1):109–22. https://doi.org/10.1109/TPWRS.2014.2320880.

[3] Apostolopoulou Dimitra, De Greve Zacharie, McCulloch Malcolm. Robust optimization for hydroelectric system operation under uncertainty. IEEE Trans Power Syst 2018;33(3):3337–48. https://doi.org/10.1109/TPWRS.2018.2807794.

[4] Bertsimas Dimitris, Sim Melvyn. The price of robustness. Oper Res 2004;52(1):35–53. https://doi.org/10.1287/opre.1030.0065.

[5] Bertsimas Dimitris, Litvinov Eugene, Sun Xu Andy, Zhao Jinye, Zheng Tongxin. Adaptive robust optimization for the security constrained unit commitment problem. IEEE Trans Power Syst 2013;28(1):52–63. https://doi.org/10.1109/TPWRS.2012.2205021.

[6] Birge John R, Louveaux François. Introduction to stochastic programming. ISBN 978-1-4614-0236-7 Springer series in operations research and financial engineeringNew York, NY: Springer New York; 2011. https://doi.org/10.1007/978-1-4614-0237-4.

[7] Blanco Ignacio, Morales Juan M. An efficient robust solution to the two-stage stochastic unit commitment problem. IEEE Trans Power Syst 2017;32(6):4477–88. https://doi.org/10.1109/TPWRS.2017.2683263.

[8] Bruninx Kenneth, Dvorkin Yury, Delarue Erik, Pandzic Hrvoje, Dhaeseleer William, Kirschen Daniel S. Coupling pumped hydro energy storage with unit commitment. IEEE Trans Sustain Energy 2016;7(2):786–96. https://doi.org/10.1109/TSTE.2015.2498555.

[9] Chazarra Manuel, García-González Javier, Pérez-Díaz Juan I, Arteseros Montserrat. Stochastic optimization model for the weekly scheduling of a hydropower system in day-ahead and secondary regulation reserve markets. Electr Power Syst Res 2016;130:67–77. https://doi.org/10.1016/j.epsr.2015.08.014.

[10] CPLEX Optimizer. Available online, accessed 16/7-2019. www.cplex.com.

[11] Dehghan Shahab, Amjady Nima, Vatani Behdad, Zareipour Hamidreza. A new hybrid stochastic-robust optimization approach for self-scheduling of generation companies: optimal self-scheduling of generating companies. Int Trans Electr Energ Syst 2016;26(6):1244–59. https://doi.org/10.1002/etep.v26.610.1002/etep.2132.

[12] Diniz Andre Luiz, Da Serra Fernanda, Costa Maria Elvira, Maceira Tiago Norbiato, Santos Dos, Lilian Chaves B, Santos Dos, Cabral Renato Neves. Short/Mid-term hydrothermal dispatch and spot pricing for large-scale systems-The case of Brazil. ISBN 9781910963104 20th Power Syst. Comput. Conf. PSCC 2018Institute of Electrical and Electronics Engineers Inc.; 2018. https://doi.org/10.23919/PSCC.2018.8442897.

[13] Farahmand H, Doorman GL. Balancing market integration in the Northern European continent. Appl Energy 2012;96:316–26. https://doi.org/10.1016/j.apenergy.2011.11.041.

[14] Gebrekiros Yonas, Doorman Gerard, Jaehnert Stefan. and Hossein Farahmand. Reserve procurement and transmission capacity reservation in the Northern European power market. Int J Electr Power Energy Syst 2015. https://doi.org/10.1016/j.ijepes.2014.12.042. ISSN 01420615.

[15] Gu Yang, Bakke Jordan, Zhou Zheng, Osborn Dale, Guo Tao, Bo Rui. A novel market simulation methodology on hydro storage. IEEE Trans Smart Grid 2014;5(2):1119–28. https://doi.org/10.1109/TSG.2013.2289915.

[16] Hart William E, Watson Jean-Paul, Woodruff David L. Pyomo: modeling and solving mathematical programs in Python. Math Prog Comp 2011;3(3):219–60. https://doi.org/10.1007/s12532-011-0026-8.

[17] Hart William E, Laird Carl D, Watson Jean-Paul, Woodruff David L, Hackebeil Gabriel A, Nicholson Bethany L, et al. Pyomo–optimization modeling in python vol. 67, 2nd ed.. Springer Science & Business Media; 2017.

[18] Helseth Arild, Fodstad Marte, Mo Birger. Optimal medium-term hydropower scheduling considering energy and reserve capacity markets. IEEE Trans Sustain Energy 2016;7(3):934–42. https://doi.org/10.1109/TSTE.2015.2509447.

[19] Helseth Arild, Mo Birger, Henden Arild Lote, Warland Geir. Detailed long-term hydro-thermal scheduling for expansion planning in the Nordic power system. IET Gener Transm Distrib 2018;120(2):441–7. https://doi.org/10.1049/iet-gtd.2017.0903.

[20] Hjelmeland Martin N, Larsen Camilla T, Korpås Magnus, Helseth Arild. Provision of rotating reserves from wind power in a hydro-dominated power system. 2016 Int conf probabilistic methods appl. to power syst IEEE; 2016. p. 1–7. https://doi.org/10.1109/PMAPS.2016.7764206. ISBN 978-1-5090-1970-0.

[21] Jaehnert Stefan, Doorman Gerard L. Assessing the benefits of regulating power market integration in Northern Europe. Int J Electr Power Energy Syst 2012;430(1):70–9. https://doi.org/10.1016/J.IJEPES.2012.05.01. ISSN 0142-0615.

[22] Jiang Ruiwei, Wang Jianhui, Guan Yongpei. Robust unit commitment with wind power and pumped storage hydro. IEEE Trans Power Syst 2012;270(2):800–10. https://doi.org/10.1109/TPWRS.2011.2169817. ISSN 0885-8950.

[23] Kazempour SJ, Moghaddam MP, Yousefi GR. Self-scheduling of a price-taker hydro producer in day-ahead energy and ancillary service markets. 2008 IEEE Canada electr power conf IEEE; 2008. p. 1–6. https://doi.org/10.1109/EPC.2008.4763320. ISBN 978-1-4244-2894-6.

[24] Kong Jiehong, Skjelbred Hans Ivar. Operational hydropower scheduling with post-spot distribution of reserve obligations. 2017 14th int conf Eur energy mark IEEE; 2017. p. 1–6. https://doi.org/10.1109/EEM.2017.7981874. ISBN 978-1-5090-5499-2.

[25] Kong Jiehong, Skjelbred Hans Ivar, Fosso Olav Bjarte. An overview on formulations and optimization methods for the unit-based short-term hydro scheduling problem. Electr Power Syst Res 2020;178. https://doi.org/10.1016/j.epsr.2019.106027. ISSN 03787796.

[26] Liu Dundun, Cheng Haozhong, Fang Sidun. Coupled stochastic and robust transmission expansion planning. 2017 IEEE power energy soc gen meet IEEE; 2017. p. 1–5. https://doi.org/10.1109/PESGM.2017.8274170. ISBN 978-1-5386-2212-4.

[27] Liu Guodong, Xu Yan, Tomsovic Kevin. Bidding strategy for microgrid in day-ahead market based on hybrid stochastic/robust optimization. IEEE Trans Smart Grid 2016;70(1):227–37. https://doi.org/10.1109/TSG.2015.2476669. ISSN 1949-3053.

[28] Löhndorf Nils, Wozabal David, Minner Stefan. Optimizing trading decisions for hydro storage systems using approximate dual dynamic programming. Oper Res 2013;610(4):810–23. https://doi.org/10.1287/opre.2013.1182. ISSN 0030-364X.

[29] Lorca Álvaro, Sun Xu Andy. Adaptive robust optimization with dynamic uncertainty sets for multi-period economic dispatch under significant wind. IEEE Trans Power

Syst 2015;300(4):1702–13. https://doi.org/10.1109/TPWRS.2014.2357714. ISSN 0885-8950.
[30] Lorca Álvaro, Sun Xu Andy. Multistage robust unit commitment with dynamic uncertainty sets and energy storage. IEEE Trans Power Syst 2017;320(3):1678–88. https://doi.org/10.1109/TPWRS.2016.2593422. ISSN 0885-8950.
[31] Lorca Á, Sun XA, Litvinov E, Zheng T. Multistage adaptive robust optimization for the unit commitment problem. Oper Res 2016;640(1):32–51. https://doi.org/10.1287/opre.2015.1456. ISSN 0030-364X.
[32] Morales Juan M, Conejo Antonio J, Madsen Henrik, Pinson Pierre, Zugno Marco. Integrating renewables in electricity markets. Volume 205 of International series in operations research & management science Boston (MA): Springer US; 2014. https://doi.org/10.1007/978-1-4614-9411-9. ISBN 978-1-4614-9410-2.
[33] Nasrolahpour Ehsan, Kazempour Jalal, Zareipour Hamidreza, Rosehart William D. A bilevel model for participation of a storage system in energy and reserve markets. IEEE Trans Sustain Energy 2018;90(2):582–98. https://doi.org/10.1109/TSTE.2017.2749434.
[34] Nord Pool. Available online [accessed 16/7-2019]. www.nordpoolgroup.com/Market-data1/Dayahead/Volumes/NO.
[35] Pandžic H, Dvorkin Y, Carrión M. Investments in merchant energy storage: Trading-off between energy and reserve markets. Appl Energy 2018;230:277–86. https://doi.org/10.1016/j.apenergy.2018.08.088. ISSN 03062619.
[36] Pozo David, Contreras Javier, Sauma Enzo E. Unit commitment with ideal and generic energy storage units. IEEE Trans Power Syst 2014;290(6):2974–84. https://doi.org/10.1109/TPWRS.2014.2313513. ISSN 08858950.
[37] Street Alexandre, Oliveira Fabrício, Arroyo José M. Contingency-constrained unit commitment with n-K security criterion: a robust optimization approach. IEEE Trans Power Syst 2011;260(3):1581–90. https://doi.org/10.1109/TPWRS.2010.2087367. ISSN 0885-8950.
[38] Street Alexandre, Brigatto Arthur, Valladão Davi M. Co-optimization of energy and ancillary services for hydrothermal operation planning under a general security criterion. IEEE Trans Power Syst 2017;320(6):4914–23. https://doi.org/10.1109/TPWRS.2017.2672555. ISSN 0885-8950.
[39] van Ackooij W, Danti Lopez I, Frangioni A, Lacalandra F, Tahanan M. Large-scale unit commitment under uncertainty: an updated literature survey. Ann Oper Res 2018;2710(1):11–85. https://doi.org/10.1007/s10479-018-3003-z. ISSN 0254-5330.
[40] Zeng Bo, Zhao Long. Solving two-stage robust optimization problems using a column-and- constraint generation method. Oper Res Lett 2013;410(5):457–61. https://doi.org/10.1016/j.orl.2013.05.003. ISSN 01676377.
[41] Zhao Chaoyue, Guan Yongpei. Unified stochastic and robust unit commitment. IEEE Trans Power Syst 2013;280(3):3353–61. https://doi.org/10.1109/TPWRS.2013.2251916. ISSN 0885-8950.
[42] Zhao Long, Zeng Bo. Robust unit commitment problem with demand response and wind energy. ISBN 9781467327275 IEEE power energy soc gen meetIEEE; 2012. p. 1–8. https://doi.org/10.1109/PESGM.2012.6344860.